The Dependence of the Initial Electron-Transfer Rate on Driving Force in *Rhodobacter sphaeroides* Reaction Centers

Arlene L. M. Haffa, Su Lin, Evaldas Katilius, JoAnn C. Williams, Aileen K. W. Taguchi, James P. Allen, and Neal W. Woodbury*

Department of Chemistry and Biochemistry, and Center for the Study of Early Events in Photosynthesis, Arizona State University, Tempe, Arizona 85287-1604

Received: March 12, 2002; In Final Form: May 14, 2002

The kinetics of the primary electron transfer following excitation of the bacteriochlorophyll dimer (P) to its lowest excited singlet state were determined for a series of reaction center mutants of *Rhodobacter sphaeroides* that have P/P^+ midpoint potentials 44−147 mV below wild type. These strains were capable of photosynthetic growth and had normal bacteriochlorophyll-to-bacteriopheophytin ratios. Decreasing the P/P^+ midpoint potential resulted in an increase in the rate constant of initial electron transfer in each of the mutants tested. At room temperature, the fastest electron-transfer time constant observed was 1.8 ps from a mutant with a midpoint potential 127 mV below wild type. The dependence of the rate on driving force in these measurements and in previous measurements of mutants with high P/P^+ midpoint potentials at room temperature was fit to a Marcus equation. Wild type was displaced approximately 100 meV from the peak of this curve. This analysis yielded a reorganization energy between 180 and 380 meV and an electronic coupling between 28 and 33 cm^{-1} depending on what value is assumed for the standard reaction free energy of initial charge separation in wild-type reaction centers. However, the temperature dependence of both wild type and the high midpoint potential mutant reaction centers is much weaker than that expected from the activation energy predicted by the Marcus formalism. In fact, an activation energy of at least 15 meV is predicted for wild type which should completely prevent electron transfer at cryogenic temperatures, yet the rate constant of initial electron transfer is increased at 10 K. One explanation for this is that certain vibrational modes that promote electron transfer in the reaction center are coupled to light absorption and are not in thermal equilibrium with the surrounding bath on the time scale of electron transfer. Thus, part of the vibrational energy required for rapid initial electron transfer may come from the absorbed photon rather than from the surrounding bath.

The photosynthetic reaction center is responsible for the conversion of light energy into a transmembrane charge separation via a series of electron-transfer reactions between its redox-active cofactors. One of the best characterized reaction centers is from the anoxygenic purple nonsulfur bacterium *Rhodobacter (Rb.) sphaeroides*. The *Rb. sphaeroides* reaction center structure has been determined and consists of three protein subunits (L, M, and H) and 10 cofactors.[1,2] The L and M subunits make up the intrinsic membrane core of the structure, with both subunits containing 5 transmembrane helices arranged in a nearly C_2 symmetric fashion. The H subunit lies predominantly on the cytoplasmic side of the intracytoplasmic membrane. Nine of the 10 cofactors, a bacteriochlorophyll dimer (P), two accessory bacteriochlorophylls B_A and B_B, two bacteriopheophytins H_A and H_B, two quinones Q_A and Q_B, and a non-heme iron (Fe), are also related by C_2 symmetry. P is near the periplasmic face of the membrane flanked by B_A and B_B on each side. H_A and H_B are farther into the membrane followed by Q_A and Q_B with the iron atom between them near the cytoplasmic side of the membrane. A carotenoid molecule is asymmetrically placed near B_B. The two sets of cofactors labeled A and B form two transmembrane chains of potential electron-transfer components. Upon excitation of P to form P*, electron transfer occurs with a time constant of a few picoseconds forming $P^+H_A^-$ presumably via $P^+B_A^-$. In about 200 ps, a subsequent electron transfer forms $P^+Q_A^-$ and then on longer time scales $P^+Q_B^-$ is formed. Under these excitation conditions in wild-type reaction centers, there is essentially no electron transfer from P to either B_B or H_B.[3,4]

The energetics of these electron-transfer reactions are determined by the midpoint potentials (E_m) of the reaction center cofactors. Cofactor midpoint potentials are mediated by the protein environment including hydrogen bonds and long-range electrostatic interactions (for reviews, see refs 5 and 6). It has previously been shown that it is possible to manipulate the midpoint potential of P over a broad range, particularly in the direction of making P harder to oxidize and thus decreasing the standard free energy change for the initial electron-transfer reaction.[7−10] These mutations progressively decrease the rate of initial electron transfer as the P/P^+ midpoint potential increases. It is also possible to stabilize the P^+ state via mutation (decrease its midpoint potential) and in so doing increase the driving force for initial electron transfer. Previously, the initial electron-transfer rate constant had only been determined for one such mutant in which histidine has been substituted for phenylalanine in the L subunit at position 168 (numbering according to refs 11 and 12 and mutant abbreviated L168HF) resulting in a roughly 95 mV decrease in midpoint potential in both *Blastochloris (Bl.) viridis* (formerly *Rhodopseudomonas viridis*) and *Rb. sphaeroides* reaction centers.[5,7,13] The rate of

* To whom correspondence should be addressed. E-mail: NWoodbury@asu.edu.

10.1021/jp0257552 CCC: $22.00
Published on Web 06/28/2002

initial electron transfer increased substantially in the mutant compared to wild type in *Bl. viridis* reaction centers, while in *Rb. sphaeroides* reaction centers the average decay of the excited singlet state of P was slightly faster than wild type.[7,13]

In both wild type and the L168HF mutant, the initial electron transfer is somewhat faster at cryogenic temperatures than at room temperatures. In wild-type reaction centers, this weak temperature dependence of the initial electron-transfer rate constant is often described in terms of electron transfer occurring near the peak of the rate vs driving force relationship where the activation energy for the reaction is zero (reviewed in ref 6). In terms of a Marcus formalism for electron transfer, this corresponds to the point in the rate vs driving force relationship where the reorganization energy and the standard reaction free energy have the same magnitude.[14] However, the results from the L168HF mutant, at least in *Bl. viridis*,[13] argue that the wild type rate may be displaced from the peak of the rate vs driving force relationship by nearly 100 meV. This is a critical point, as application of standard electron-transfer theory would predict that such a displacement should give rise to a substantial activation energy for electron transfer in wild-type reaction centers, preventing rapid charge separation at low temperatures. However, the rate constant of initial electron transfer at 10 K is more than twice the room-temperature value.[15]

The argument made above for a substantial displacement of wild type from the peak of the rate versus driving force relationship presupposes that the increase in rate constant observed in L168HF reaction centers is due to the increase in the standard reaction free energy of initial charge separation that occurs upon decreasing the P/P^+ midpoint potential. On the other hand, it is also possible that the L168HF mutation changes the electronic coupling in the system, and that these secondary effects give rise to the increase in the electron-transfer rate constant in the mutant. Support for a significant change in the structure of the mutant relative to wild type, which could in turn affect coupling, comes from the fact that the L168HF mutation results in the loss of a hydrogen bond to the ring A acetyl group of the A side bacteriochlorophyll of P (P_A). Structural data shows that the acetyl group has rotated 1.1 angstroms closer to the Mg^{2+} center of the other bacteriochlorophyll that comprises P (P_B) in the mutant.[16]

To settle the question of whether wild-type reaction centers are at the peak of the rate vs driving force relationship, and to better understand how the midpoint potential of P affects initial electron transfer, a series of mutants, not all involving hydrogen bond disruption as the L168HF mutant does,[16] were designed to stabilize P^+ and thus increase the standard free energy change for initial charge separation. Specifically, these mutations involve placing a potentially negatively charged amino acid residue in close proximity to the dimer, either in the L168 position (L168HE) or at points that should not directly affect the hydrogen bonding between P and the protein environment (L170ND and M199ND). These three single mutants and the four possible double and triple mutants have been constructed and characterized. The P/P^+ midpoint potentials for this set of mutants have been reported in a separate publication.[17] Between these mutants and previously characterized high P/P^+ midpoint potential mutants, a range of midpoint potentials covering almost 410 mV is now accessible, allowing the variation of the driving force for initial electron transfer from nearly 150 meV less than wild type to about 260 meV more than wild type. This allows the construction of a rate vs driving force relationship that extends substantially in either direction from wild type, making it possible to determine whether wild type is at the peak of the relationship between rate and driving force or, if not, how far it is displaced.

It is also possible to investigate another aspect of reaction center electron transfer that is of current interest using the low P/P^+ potential mutants. A number of different studies have now argued convincingly that the primary reason electron transfer proceeds almost exclusively from P* via the A-cofactor branch rather than the B-branch of cofactors in the reaction center is that the state $P^+B_B^-$ is above P* in free energy while $P^+B_A^-$ is at or below the standard free energy of P*.[18−20] This suggests that by lowering the P/P^+ midpoint potential far enough, the state $P^+B_B^-$ should drop below P* in free energy, possibly allowing B-side charge separation to occur. Transient absorption measurements designed to detect B-side electron transfer in this series of mutants are described.

Materials and Methods

Strain Construction and Characterization. The mutagenesis system and deletion strains of *Rb. sphaeroides* have been previously described.[21−23] To facilitate the isolation and purification of reaction centers, a poly-histidine tag (His-tag) was engineered at the carboxy-terminus of the M subunit, as previously published,[24] except that the additional screening mutation introduced previously was not incorporated. The measurements of the mutants reported here were compared to wild-type His-tagged reaction centers under the same conditions. The isolated reaction centers had an A_{280}/A_{800} ratio of <1.5 and were prepared in 15 mM tris(hydroxymethyl)aminomethane-HCl (Tris-HCl), 0.025% lauryldimethlyamine-*N*-oxide (LDAO), 1 mM (ethylenediamine)tetraacetic acid (EDTA), 150 mM NaCl buffer pH 8 (TLE + 150 mM NaCl). Bacteriochlorophyll/bacteriopheophytin pigment ratios were determined via extraction using acetone:methanol 7:2.[25,26] The determination of the P/P^+ midpoint potentials of the low potential mutants is described elsewhere.[17] Photosynthetic growth was tested in 0.3% Bacto Peptone/0.3% Bacto Yeast Extract/1.6 mM $MgCl_2$/1 mM $CaCl_2$/1% Bacto Agar. This was accomplished by growing a single colony in liquid culture to late log phase and then using a sterile stick to inoculate an agar stab culture. Culture tubes were capped, illuminated using a locally built light box equipped with two 40 W tungsten light bulbs and monitored for one week for photosynthetic growth.

Absorption Spectroscopy. Ground-state absorption spectra (240−1000 nm) of isolated reaction centers in TLE + 150 mM NaCl were measured with a Cary V spectrophotometer (Varian) at 295 K in a 1 cm quartz cuvette with 1 nm spectral resolution.

The apparatus used for transient absorption spectroscopy with subpicosecond time resolution has been described previously.[27] The continuum probe beam was polarized at the magic angle (54.7 °) with respect to the excitation pulse. The excitation was tuned to a wavelength of either 860, 850, or 840 nm depending on the position of the P band at room temperature (see Figure 1A) and the full-width-at-half-maximum of the excitation spectral profile was 5 nm with a temporal duration of ∼100 fs. For room-temperature experiments, 1 mM 1,10-ortho-phenanthroline was added to reaction centers in TLE + 150 mM NaCl to block Q_A to Q_B transfer, and the sample was then placed in a spinning wheel with an optical path length of 2.5 mm. An optical density (OD) of roughly 1.0 in the wheel at 800 nm was used for most mutants. However, reaction centers containing the L168HE mutation required an OD of 1.6 or greater in order to achieve a sufficient absorbance change amplitude. For measurements at 10 K, the quinones were removed as previously described.[28] Reaction centers in TLE + 150 mM NaCl were

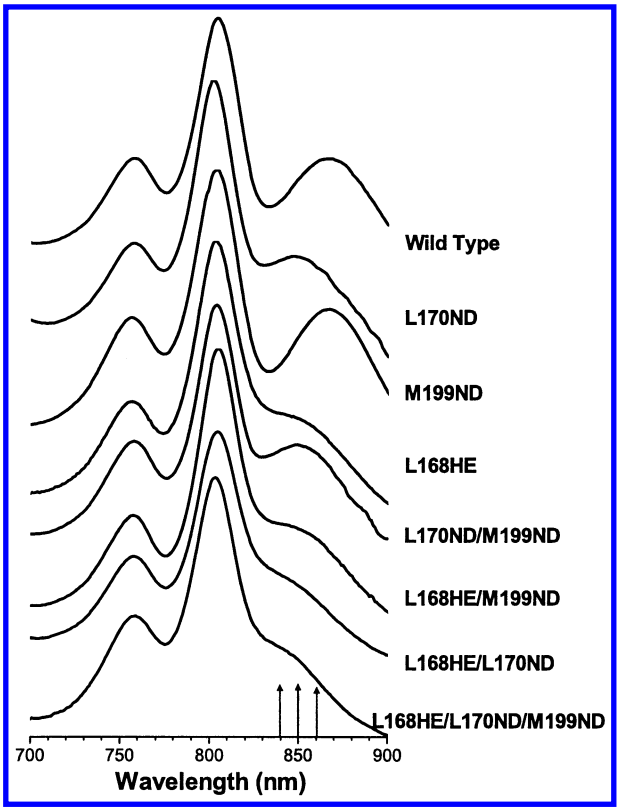

Figure 1. Ground-state optical absorption spectra of wild type, L170ND, M199ND, L168HE, L170ND/M199ND, L168HE/M199ND, L168HE/L170ND, and L168HE/L170ND/M199ND mutant reaction centers shown in order of decreasing P/P^+ midpoint potential. Spectra were taken at room temperature in a 1 cm quartz cuvette. The arrows on the *x* axis indicate the center wavelength of the excitation pulse used in the transient absorption measurements. Excitations at 840 and 850 nm were used for the L168HE/L170ND/M199ND and L168HE/L170ND reaction centers, respectively, and all others were excited using 860 nm excitation. The spectra were normalized at the peak of the monomer bacteriochlorophyll band near 800 nm in each case. The curves are offset for ease of comparison.

mixed 1:2 (v:v) with glycerol, degassed and placed between two quartz plates with an O-ring spacer of 1.2 mm, then attached to the coldfinger of a closed circulated helium displex (APD) and cooled. Difference transient absorption spectra were recorded for wild type and each of the mutant reaction centers from 480 to 1025 nm (two sets of data from 480 to 780 and 730 to 1025 nm were acquired). First, 110 difference absorption spectra were measured at 100 fs intervals between −1 and 10 ps and then an additional 60 difference spectra were measured at 10 ps intervals extending the time scale to 610 ps. Spectral dispersion at early times was corrected empirically using measurements of instantaneous CS_2 birefringence[29] and data analysis of the transient absorbance surfaces (time vs wavelength) was performed as previously described by global fitting to a sum of 2 exponential decay terms and a constant.[30]

Results

A series of *Rb. sphaeroides* reaction center mutants have been generated in which the amino acid residues near the dimer have been altered to stabilize the P^+ state and thus decrease the midpoint potential of P.[17] This series is comprised of three single mutants (the specific mutations were L168HE, L170ND, and M199ND), the three possible double mutants made by combining these mutations (L168HE/L170ND, L168HE/M199ND, and L170ND/M199ND), and the triple mutant formed by combining all three mutations (L168HE/L170ND/M199ND). At pH 8.0, the P/P^+ midpoint potential in these mutants ranged from 44 to 147 mV below wild type (Table 1). The measurements described below were all performed at pH 8.0. All three mutations place ionizable residues near the dimer. The mutation L168HE additionally may remove a hydrogen bond from one of the ring A acetyl groups of the dimer, which has also been shown to decrease the midpoint potential of P.[7,13] All strains were capable of photosynthetic growth, and the bacteriochlorophyll:bacteriopheophytin pigment ratios indicated that all mutants had a full complement of bacteriochlorophyll and bacteriopheophytin (extraction analysis gave bacteriochlorophyll:bacteriopheophytin = 1.87 ± 0.09 with a range of 1.70−1.95 in the different mutants compared to 1.96 for wild type using identical procedures and solvents).

Ground-State Absorption Spectra. The ground-state optical absorption spectra of wild-type and mutant reaction centers were measured at room and cryogenic temperatures. The most notable differences between mutant and wild-type reaction center ground-state spectra are in the peak positions of the Q_y transition of the Bchl dimer (P), particularly for the L subunit mutants (Figure 1). In a number of these mutants, the peak position of the Q_y transition of P is shifted far enough to the blue so that it is essentially a shoulder of the 800 nm band of the monomer bacteriochlorophylls. For this reason, the quantitative peak position of the P transition in each of the mutants was determined from the nondecaying component of the decay associated spectra resulting from fits of the transient absorption data (see below and Figure 2D−F). Determined in this way, the peak absorbance of the Q_y transition of P ranges from 838 to 865 nm at room temperature compared to 861 nm for wild type (Table 1). The mutations L168HE and L170ND produce shifts toward higher energy of 14 and 12 nm, respectively, in this transition. The mutation M199ND results in a 4 nm spectral shift to lower energy. In the double and triple mutants the shifts are determined predominantly by the L-side mutations, with the largest shifts occurring in mutants with multiple L-side mutations. The Q_x spectral region is essentially the same in the wild-type and the mutant reaction centers, with only very small (1−2 nm) shifts in absorption peaks (data not shown).

The peak of the Q_y absorption transition of P ranged from 870 to 898 nm at 10 K compared to 894 nm for wild type with the shifts following the same trends as those reported above for room temperature (data not shown). In addition, the shoulders evident on the red side of both the 600 and 800 nm absorption bands in wild type at 10 K cannot be distinguished from the main bands in any of the mutants except for M199ND which looks similar to wild type.

Transient Absorption Spectroscopy. With the exception of the position of the ground-state bleaching associated with P, both the time-resolved spectra and the decay associated spectra resulting from fits to two exponential decay terms and a constant were very similar in mutant and wild-type reaction centers (examples are given in Figure 2). In addition, the time course of the absorption changes associated with the H_A to Q_A electron-transfer reaction were similar to those seen in wild type (roughly 200 ps), though detailed kinetics on this time scale were not extensively studied.

All of the mutants with lower P/P^+ midpoint potentials than wild type resulted in time constants for decay of P* and appearance of the resulting charge-separated state that were faster than those observed for wild type. The fastest electron-transfer time constant observed was 1.8 ps and was measured in a mutant with a P/P^+ midpoint potential about 127 mV below

TABLE 1: Characteristics of the Low P/P$^+$ Mutants

strain[a]	P/P$^+$ ΔE_m, mV[b]	peak absorption wavelength of P, nm[c]	change in transition energy of P,meV[d]	ΔG^0_R, meV[e]	τ_1, ps[f]
wild type	0	861	0	0	3.1
L170ND	−44	849	20	−64	2.1
M199ND	−48	865	−7	−41	2.9
L168HE	−75	847	24	−99	2.1
L170ND/M199ND	−83	849	20	−103	2.5
L168HE/M199ND	−110	845	27	−137	2.2
L168HE/L170ND	−127	839	38	−165	1.8
L168HE/L170ND/M199ND	−147	838	41	−188	2.1

[a] Numbering and nomenclature as described in text. First letter refers to the protein subunit followed by amino acid numbering according to refs 11 and 12. The letters following the numbers refer to the residues in the native protein and replacements in the mutant strains. [b] Change in P/P$^+$ midpoint potentials relative to wild type (P/P$^+$ ΔE_m) ± 5 mV, previously published.[50] [c] Determined from the nondecaying component of the decay associated spectra such as those shown in Figure 2. [d] Calculated using column 3 with the assumption that the P ground state has not shifted. [e] Combines information in columns 2 and 4 to generate an estimate of the change in reaction free energy relative to wild type assuming a one-electron process. [f] Fast component lifetime from the global fits of the transient absorption data (examples given in Figure 2). Error estimate is ±0.2 ps.

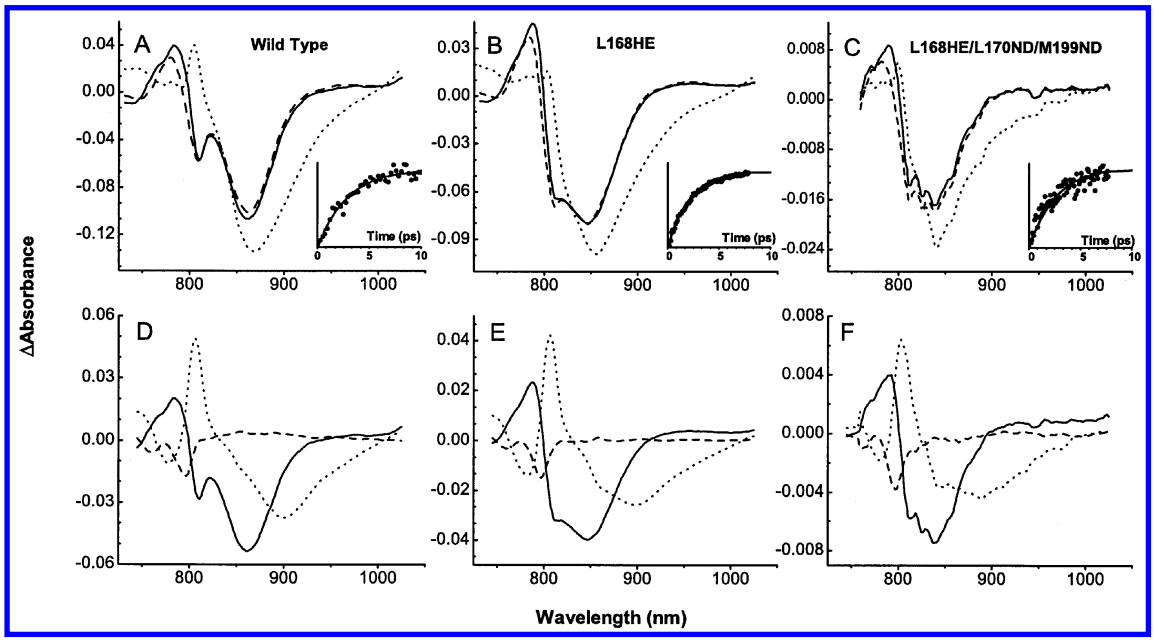

Figure 2. A−C: time-resolved absorption difference spectra; (•••) 0 ps, (--) 17.3−18.7 ps, and (—) 589−608 ps. The transient spectra shown were reconstructed from the fits to correct for spectral dispersion at early times. Insets: the decay of the stimulated emission monitored at a wavelength 65 nm to the red of the peak positions of the Q_y transitions for P given in Table 1. D−F: the decay associated spectra of (• •) the shortest component (2.1−3.1 ps), (- -) the intermediate component (approximately 200 ps), and (—) the nondecaying component. Data arranged in columns by type of reaction center from left to right: wild type, L168HE, and L168HE/L170ND/M199ND. Excitation was in the P band in each case as shown in Figure 1.

wild type (Table 1). In general, the time constant for initial electron transfer decreases from 3.1 ps in wild type to about 2.0 ps in the low potential mutants, where it reaches a plateau, at least within the midpoint potential range and time constant variation of the mutants measured. The kinetics of P* decay for several of the mutants are also shown in the insets in Figure 2A−C. Whether one does a global analysis (fitting all the absorption changes at all wavelengths simultaneously) or analyzes specific wavelengths which include changes due to P* decay (the P* stimulated emission region to the red of 900 nm), the conclusion remains the same: initial electron transfer occurs more rapidly in all of the mutants with decreased P/P$^+$ midpoint potentials than it does in wild type.

One possible explanation for the increased initial electron-transfer rate constants in the low potential mutants could be that an additional electron-transfer pathway has opened up that utilizes the B-side reaction center cofactors. It is known from several studies that stabilizing $P^+B_B^-$ can result in an increased rate of electron transfer along the B side.[18,20,31] It therefore seems possible that by decreasing the P/P$^+$ midpoint potential in the mutants described here, $P^+B_B^-$ has been driven below P* in free energy and could provide an alternate decay path for P*. To investigate this possibility, transient absorption spectra were taken in the Q_x region at room temperature for all of the mutants and at 10 K for wild type and the L168HE and L168HE/M199ND mutants. The 530 and 540 nm absorption bands (corresponding to H_B and H_A absorbance, respectively) are resolved at low temperature, and as little as 10% B-side electron transfer can be detected under these conditions. At room temperature, band broadening results in greater overlap, and this increases the error in the ability to distinguish between pathways. No evidence for involvement of H_B was observed in the electron-transfer reactions at either temperature in any of the mutants (data not shown).

Low-temperature measurements were also performed in the Q_y region for L168HE in order to determine if the rate constant of electron transfer would decrease with decreasing temperature in a mutant in which the electron-transfer rate was near the peak

of the rate vs free energy curve (in wild-type reaction centers, the rate constant decreases by more than a factor of 2 at 10 K compared to room temperature). The L168HE mutant's initial electron-transfer rate constant decreased by roughly the same proportion as does wild type, resulting in a time constant at 10 K of 0.9 ps compared to 1.2 ps for wild type at this temperature using similar time scales and analysis. Thus, L168HE not only speeds up with decreasing temperature but it remains faster than wild type at 10 K by nearly the same factor as at room temperature.

Discussion

Past work has demonstrated that the midpoint potentials of reaction center redox cofactors depend strongly on interactions with the amino acids that make up their local environments.[13] The P/P^+ midpoint potential of the bacterial reaction center can be altered over a range of 147 mV below to 260 mV above wild type by the introduction of 1−3 point mutations while still maintaining a quantum yield of primary charge separation greater than or equal to 50% at room temperature. Larger midpoint potential increases above the wild-type value have been created, but the quantum yield becomes lower[32] (and unpublished results). The mutations resulting in midpoint potential changes in the −147 to +260 mV range (relative to wild type) are not sufficiently deleterious to keep the reaction center from supporting photosynthetic growth and pigment ratios are not altered in these reaction center mutants. The predominant effect of the mutations is apparently on the energetics of the charge-separated states.

The P/P^+ Midpoint Potential Is Not Strongly Correlated with the Spectral Changes of P. The most prominent ground-state spectral change in the low P/P^+ midpoint potential mutants described in this work are the blue shifts of the Q_y transition of P observed in the L subunit mutants (Figure 1). The magnitude and the direction of these shifts are similar to that previously found for L168HF mutant reaction centers.[7] The M subunit mutation (M199ND) results in a slight red shift. Comparison of the optical spectra (Figure 1) or the peak wavelength positions (Table 1), shows that there is no apparent correlation between midpoint potential and spectral shift. The conclusion that the midpoint potential of P is not strongly correlated with the energy of its lowest absorption transition is in line with previous results from high potential mutants.[5,7−10] Instead, it appears that each of the different single mutations has influenced the P near-infrared transition differently and independently of midpoint potential and that the multisite mutants represent combinations of the effects of the single mutations. For example, the M199ND mutation results in a small red shift of the P to P* Q_y transition, and yet it has a larger midpoint potential change relative to wild type than does the L170ND mutation which shifts the P band more than 10 nm to the blue (Figure 1 and Table 1).

It is interesting that the M199ND and L170ND mutations affect the spectrum of P so differently given their symmetry related positions (M199 is related by the approximate C_2 symmetry of the reaction center to L170). By titrating the midpoint potential of the M199ND mutant, it has been found that the pK_a of the aspartic acid at M199 in the mutant is 7.9.[17] The midpoint potential of the symmetry related L170ND mutant has been measured at two pHs and gives results similar to M199ND. It is likely that these two residues have similar pK_a values and are therefore partly charged at pH 8.0, the pH used in the present study. Since there is apparent similarity in the protonation state, and thus the charge, of the aspartic acids at L170 and M199 in the mutants and nearly equal distances between either L170 or M199 and P, the different effects of the two mutants on the Q_y transition of P presumably reflect asymmetry in this transition.[33] It is possible that these mutations alter the energy of the charge transfer states that contribute to P* and thus the extent to which these states mix into P*.[34,35] The L168HE mutation is somewhat different from either of the other two in that it shifts both the wavelength and the oscillator strength of the P band. In addition to introducing a potentially charged residue in the vicinity of P as the other mutations do, the L168HE mutation may involve removing a hydrogen bond between the protein and P (it is not clear if the glutamic acid residue forms a hydrogen bond or not in this mutant) possibly rotating the ring A acetyl group of P_A, as observed for the L168HF mutant.[36] When the midpoint potential of this mutant was measured at several pH values between 6 and 9.5, the pK_a of the glutamic acid was found to be roughly 7.7 (unpublished results). At the pH of 8.0 where the measurements were taken, this residue is presumably partially protonated.

Lowering the P/P^+ Midpoint by 147 mV Does Not Allow B-Side Electron Transfer To Compete with A-Side Transfer. Recent measurements of B-side electron transfer in bacterial reaction centers have shown that the dominant factor in determining the rate of electron transfer along the B branch from P* is most likely the relative free energy of the initial excited state and the state $P^+B_B^-$.[18,31,37−39] For example, a decrease in the energy of $P^+B_B^-$, by converting B_B to a bacteriopheophytin, results in rates of B-side electron transfer comparable to that on the A side.[20] Measurements using such a mutant have resulted in an estimate of the $P^+B_B^-$standard free energy that places it roughly 100 ± 70 meV above P*.[20] It seems reasonable to suspect that by dropping the P/P^+ potential by nearly 150 mV, it might be possible to lower $P^+B_B^-$relative to P* enough to allow rapid B-side electron transfer to occur.

Transient absorption spectroscopy in the series of low potential mutants described here reveals that the overall spectral signatures of the electron-transfer intermediates in these reaction centers in both the Q_x (data not shown) and Q_y (examples given in Figure 2) regions of the reaction center spectrum are similar to those observed using wild type. No evidence for formation of either B_B^-or H_B^- at room temperature was observed, but it is difficult to detect small yields of B-side electron transfer at room temperature due to the overlap between the spectral transitions of the A and B cofactors. Measurements in the Q_x region of the spectrum at low temperature where the H_A and H_B Q_x transitions are well resolved show no indication of electron transfer along the B side to H_B in L168HE or L168HE/M199ND RCs upon direct excitation of P.

Apparently, B-side electron transfer in these mutants is not fast enough to compete effectively with A-side transfer. There are at least two possible reasons why lowering the midpoint potential of P substantially may not result in observable B-side transfer in these mutants. First, some of the negative charges that stabilize P^+ may well destabilize B^- and thus the full effect of the stabilization may not be felt. Second, as shown in Table 1 and described below, A-side electron transfer speeds up substantially in these mutants, making the competing B-side reaction more difficult to detect. At 10 K, a temperature that permits spectral resolution between the two bacteriopheophytin peaks, the rate constant for A-side electron transfer is increased not only in these mutants, but also in wild type. The minimal detectable yield of B-side electron transfer for our system is ∼10%. This means that to be observable, the time constant for B-side electron transfer would have to be as fast or faster than ∼10 ps at 10 K. This is approximately the time constant for

B-side electron transfer at room temperature in a mutant in which the ligand for B_B has been replaced with a nonliganding amino acid, and a bacteriopheophytin occupies the B_B site instead of bacteriochlorophyll (the so-called ϕ_B mutant).[18,20] In this case, the initial B-side charge-separated state should be stabilized by roughly 250 meV due to the difference in the midpoint potentials of bacteriochlorophyll and bacteriopheophytin. The 150 meV stabilization expected for $P^+B_B^-$ in the series of mutants described here may not be sufficient to achieve a B-side electron-transfer rate that competes well enough with A-side transfer to be detectable. Possibly by combining these mutations with additional mutations that slow A-side transfer, or with the so-called β mutant which makes the H_B ground state bleaching easier to observe at room temperature, B-side transfer might be able to compete effectively enough to be observed (see, for example, refs 31, 38, and 39). As will be described in a later publication, it is possible to generate B-side electron transfer forming a long-lived H_B^- state at room temperature in at least one of these mutants (L168HE/L170ND) by exciting the monomer bacteriochlorophylls or the bacteriopheophytins directly (740 or 800 nm), though when this higher energy excitation of the mutant is used, B-side charge separation likely does not involve electron transfer from P*.

The Rate vs Free Energy Relationship for A-Side Electron Transfer. The initial charge separation time constant for A-side electron transfer speeds up with decreasing potential and then plateaus at about 2 ps (Table 1). The fastest mutant (L168HE/L170ND) has a time constant for electron transfer that is decreased by 45% relative to wild type. This trend is consistent with previous work on the L168HF mutation, particularly as it has been studied in *Bl. viridis*.[13] In this mutant, the midpoint potential of P was found to be 80 mV below wild type and the primary charge separation time was found to decrease from 3.5 ps in wild type to 1.1 ps in the *Bl. viridis* mutant. In *Rb. sphaeroides*, the L168HF mutant also shows a slight increase in the average electron-transfer rate.[7] One of the questions raised by the studies of the original L168HF mutant is whether the observed increase in electron-transfer rate was actually due to changes in charge-separation energetics or due to other changes (distances and/or orientations) caused by altering the hydrogen bonding pattern in the mutant. In the work described here, three different mutations that decrease the midpoint potential of P were compared, both individually and in combination. One of these was a different L168 mutant and the other two were mutants whose effects on energetics should be due to primarily electrostatic interactions. In each case, an increase in the rate constant for initial electron transfer is observed (Table 1) implying that lowering the midpoint potential of P, and therefore, increasing the driving force for initial charge separation, does indeed result in faster initial electron transfer.

By combining the results from low P/P^+ potential mutations measured in this report with high midpoint potential mutants studied previously, a rate versus driving force relationship can be generated that extends from about 150 meV below to 260 meV above the driving force for initial charge separation in wild type (Figure 3). In Figure 3, the rate of initial electron transfer is plotted as a function of the relative standard reaction free energy (ΔG_R^0) for each mutant reaction center. The relative standard reaction free energy is defined as the difference in the standard reaction free energy for initial electron transfer between each of the mutants and the wild type, thus, wild type is shown at 0 meV in Figure 3. In determining this relative free energy change, it was assumed that the P/P^+ midpoint potential is the only relevant midpoint potential that changes and that

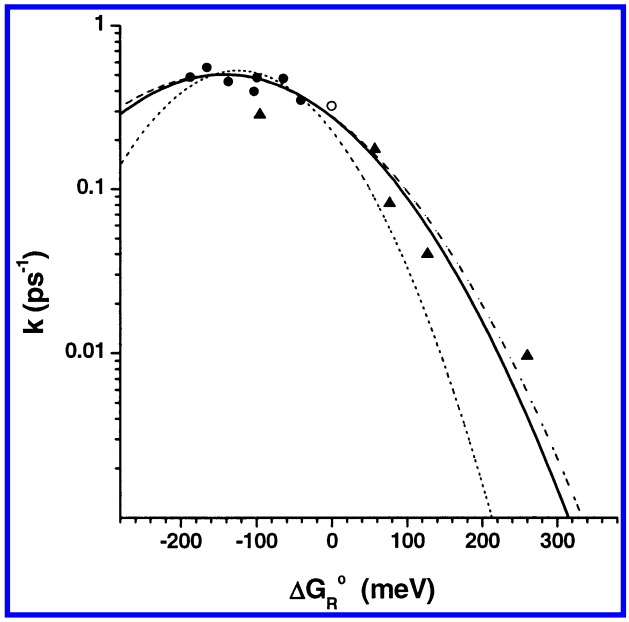

Figure 3. The relationship between the initial electron-transfer rate and ΔG_R^0, the standard reaction free energy for initial electron transfer relative to wild type. The current data from the low potential mutants studied here are shown as closed circles (●), see Table 1. Data from previously published results[7,9,55,62] on other mutants are shown as closed triangles (▲). The wild-type rate constant from the current study using 860 nm excitation is shown as an open circle (○). For the fits to the Marcus equation shown, the driving force for wild-type reaction centers was either set to −200 meV (—), or −60 meV (· ·) or allowed to freely vary freely in the fit resulting in a value of −230 meV (· —). See text for details.

the degree to which it changes between the wild type and each mutant is the same on the picosecond time scale as it is on the minute time scale of electrochemical midpoint titrations. The relative free energy changes shown also take into account the change in the P → P* transition energy estimated from the shift in the peak of the Q_y transition of P in the mutants relative to wild type (Table 1). This effect is as large as 40 meV in some mutants, and should be reflected in the overall standard free energy change for charge separation from P*, assuming that the ground state energy remains unchanged in the mutants and only the excited-state energy changes.

There are a couple of points regarding mutants in Figure 3 from past studies that should be noted.[7−10] For the HF(L168) mutant, the time interval used in collecting data was 500 fs rather than 100 fs as it is in this study. This resulted in a P* decay time for wild type of 3.8 ps instead of the 3.1 ps time obtained here. Thus, the 3.6 ps time reported for the HF(L168) mutant is undoubtedly long in comparison to times shown for mutants in the present analysis.[7] This mutant has been included in Figure 3 for completeness, but it has not been included in the fit described below. In some of the high P/P^+ midpoint potential mutants, the yield of initial electron transfer is not unity.[8,9] In most cases, the yield losses were relatively small (20−30%) and the measured P* decay times are used directly in Figure 3. However, in the case of the highest potential mutant (L131LH/M160LH/M197FH), the yield of charge separation is only about 50%. Thus the actual electron-transfer rate constant is about half of the value measured for the decay rate constant of the excited singlet state of the donor. Thus, for this mutant, the corrected value of the electron-transfer rate is shown in Figure 3 and used in the fitting below.

The data plotted in Figure 3 show that there is a clear correlation between the rate constant and the estimated driving

force for initial electron transfer in these mutants. The rate of charge separation reaches a maximum with decreasing P/P^+ midpoint potential, possibly even declining at the lowest value of the midpoint tested, though the slight decrease could be due to reasons other than the midpoint change. It is also clear that wild type is not at the maximum of the rate vs driving force relationship, but is situated nearly 100 meV in standard reaction free energy away. This is consistent with previous measurements on the L168HF mutant in *Bl. viridis*.[7,13] Depending on what one takes as the standard free energy of the initial charge-separation event, 100 meV could be a very significant energetic difference. For example, the standard free energy difference for the reaction $P^* \leftrightarrow P^+B_A^-$ has been estimated to be in the range of −60 to −100 meV (see, for example, refs 39−41). If one assumes that this is the reaction being probed in the rate vs driving force relationship, then the optimum standard free energy difference for this reaction is actually −160 to −200 meV, a factor of two to three greater than the wild-type value.

A mechanistic interpretation of this rate vs free energy relationship requires the application of a model and its associated assumptions. There are various electron-transfer theories that can be applied to fit the data in Figure 3. However, at room temperature, for driving force values less than or equal to the driving force at the peak of the rate versus driving force relationship, the inclusion of multiple vibrational modes[42] or quantum corrections[43] makes relatively little difference in the outcome (calculations not shown). Thus, a simple formalism will be applied to give a rough idea of the types and values of parameters involved and to determine if the assumptions inherent in these models give consistent results.

Electron-transfer reactions, as described by Marcus,[14] are controlled by a term containing the activation energy for the reaction and a term containing the coupling between donor and acceptor. The activation energy in the simplest case is determined by the driving force (defined as the standard free energy difference between P* and the charge-separated state) and the reorganization energy of the system. The data of Figure 3 were fit to the Marcus equation[14] in the form

$$k = \frac{2\pi}{\hbar} H_{DA}^2 (4\pi\lambda k_B T)^{-(1/2)} \exp\left[- \frac{(\Delta G^0_{wt} + \Delta G^0_R + \lambda)^2}{(4\lambda k_B T)} \right] \quad (1)$$

where k is the rate constant for electron transfer, k_B is the Boltzman constant, T is the temperature, H_{DA} is the electronic coupling element between the donor and the acceptor, λ is the reorganization energy, ΔG^0_{wt} is the standard free energy change for initial electron transfer in wild type, and ΔG^0_R is the difference between the standard free energy change for initial electron transfer in wild type and the mutant (the abscissa of Figure 3).

In this report, it is the energetics that is systematically being varied ($\Delta G_R{}^0$ in Table 1 and Figure 3), and thus in modeling the data of Figure 3, it will be assumed that the electronic coupling is not systematically changing among the mutants tested. The reorganization energy is also assumed to be constant as a function of the mutation. The latter two assumptions seem reasonable in that it is not clear why either electronic coupling or reorganization energy would change systematically in the series of mutants used, though some of the mutant to mutant fluctuation in rate constants may be due to changes in these parameters. Marcus theory also involves inherent assumptions (for example, instantaneous thermal equilibration with the bath of the vibrational mode coupled to electron transfer, as will be discussed below).[44]

To use eq 1, one must either know the standard free energy change associated with charge separation in wild-type reaction centers (ΔG^0_{wt}) or allow this to vary as a free parameter in the fit to the equation. Both approaches have been used here (Figure 3). If one assumes that the initial reaction is electron transfer from $P^* \leftrightarrow P^+B_A^-$, the corresponding standard free energy difference for the wild-type reaction is thought to be between −60 meV and −100 meV (see, for example, refs 39−41). If one holds the value for wild type constant at −60 meV, the fit yields a value of 180 meV (1452 cm^{-1}) for the reorganization energy of the initial electron-transfer reaction and 3.5 meV (28 cm^{-1}) for the electronic coupling constant. On the other hand, the overall reaction $P^* \leftrightarrow P^+H_A^-$ has a standard free energy change for wild type in the range −150 to −280 meV.[39,45−50] Using −200 meV for wild type, the fit for the reorganization energy of the initial electron-transfer reaction yields 340 meV (2742 cm^{-1}) and the overall electronic coupling element between the donor and acceptor is found to be 4.0 meV (32 cm^{-1}). Also shown is a fit in which $\Delta G_{wt}{}^0$ was allowed to vary freely, resulting in a value of −230 meV for this parameter. Allowing ΔG^0_{wt} to vary freely results in values of 380 meV (3065 cm^{-1}) and 4.1 meV (33 cm^{-1}) for the reorganization energy and electronic coupling, respectively.

A wide range of estimates of the reorganization energy and electronic coupling parameters for initial electron transfer have been published previously. For example, in a model that uses high-frequency nuclear modes and a superexchange electron-transfer mechanism at room temperature, a reorganization energy in the range 800 ± 250 cm^{-1} (100 ± 30 meV) and an electronic coupling term of 20 cm^{-1} (2.5 meV) was found.[40] Using the same data, but a modified model without high-frequency nuclear modes, and a sequential electron-transfer mechanism,[51] the reorganization energies of the two electron-transfer events (P → B and B → H) were both found to be 98 meV (790 cm^{-1}) with an overall reorganization energy of 198 meV (1597 cm^{-1}), and the two electronic coupling terms were found to be equal at 2.8 meV (22.6 cm^{-1}). In this model the rate of electron transfer is predicted to drop dramatically for driving forces larger than 250 meV. These are only a couple of examples of past estimates and additional studies have been reviewed elsewhere.[52] The reorganization energy values estimated here from the fit of the rate vs free energy relationship in Figure 3 are larger than most past estimates. This arises from the fact that the peak of the curve has been shifted from the wild-type driving force value to a driving force substantially larger than wild type, increasing the displacement and thus the reorganization energy.

Marcus electron-transfer theory predicts that the rate vs driving force relationship should substantially narrow with decreasing temperature, resulting in much lower rates far from the peak and a slight increase in rate at the peak of the curve.[53] The activation energy (E_A) for wild-type reaction centers can be calculated as

$$E_A = \frac{(\Delta G^0_{wt} + \lambda)^2}{(4\lambda)} \quad (2)$$

Using −230 meV for ΔG^0_{wt} and 380 meV for λ, which is the most permissive condition generated in the fit of Figure 3, yields an E_A of 15 meV for wild-type reaction centers and much greater activation energies for the higher midpoint potential mutants. Using −60 meV for ΔG^0_{wt} and 180 meV for the reorganization energy gives an activation energy of 20 meV for wild type. Either activation energy should completely prevent electron transfer at cryogenic temperatures in wild type and all the high

midpoint potential mutants (k_BT at 10 K is 0.9 meV). However, the rate constant for electron transfer in wild-type reaction centers increases with decreasing temperature and the high midpoint potential mutants used here still undergo electron transfer at low temperature to at least a measurable extent.[9,10] Clearly the activation energy predicted by applying Marcus theory and its associated assumptions to the data in Figure 3 is not consistent with the observed temperature dependence of initial electron transfer.

It is possible that there are changes in the protein structure at lower temperatures,[54] or that the activation energy is temperature dependent[42] (due, for example, to a temperature-dependent P/P^+ midpoint potential). However, it is somewhat difficult to imagine that these effects could almost exactly cancel the several million fold decrease in the rate constant of electron transfer expected at cryogenic temperatures given the 15−20 meV activation energy estimated above for wild-type reaction centers. The high potential mutants should have even larger activation energies, and should not undergo electron transfer at all at low temperature, contrary to observation.[9,55] Part of the explanation for this apparent inconsistency could lie in the inherent static and dynamic heterogeneity of charge-separated state energetics, though a large distribution in free energies should result in a lower quantum yield of charge separation at low temperature for wild type, given a substantial activation energy, and this is not observed. One also has to be concerned about the accuracy of the driving force estimates. It is not clear that the midpoint potential differences measured between wild type and mutants on the minute time scale have the same magnitude on the picosecond time scale. In addition, the low midpoint potential mutants studied here involve ionizable amino acids and have pH dependent midpoint potentials.[17] At the pH values used in this study, the protonation state of the reaction center would be heterogeneous with regard to these amino acids on the picosecond time scale, and this could also result in inaccuracies in the estimate of the driving force from the average midpoint potential. However, for wild type and a number of the high potential mutants, the dependence of the P/P^+ midpoint potential on pH is weak (refs 56 and 57 and unpublished data), and thus any heterogeneity in protonation state is unlikely to have a major effect on the P/P^+ midpoint potential of these reaction centers. Also the original low potential mutant, L168HF, involves the introduction of a phenylalanine, and this residue is not protonatable. It is also possible that negative charges introduced to stabilize P^+ in some of the mutants destabilize somewhat the anion partner of P^+ upon charge separation (though for at least some of the mutations, the distances involved should make such effects small). Though any of these effects could shift the free energy of certain mutants in Figure 3 to some extent, it is difficult to see how this would change the overall result that wild type is not at the peak of the rate vs driving force relationship, and thus wild-type reaction centers and all the mutants with higher P/P^+ midpoint potentials than wild type should have substantial activation energies.

One possible explanation for the weak temperature dependence of the initial electron-transfer rate in wild type and the high potential mutants that is consistent with the data of Figure 3 is that electron transfer occurs from a vibrationally unrelaxed state, even when direct excitation of P is used. If the optical transition results, directly or indirectly, in excitation of a vibrational mode that in turn is coupled to electron transfer, this may provide the energy needed to overcome the activation barrier rather than relying on energy from the thermal bath. This concept is consistent with recent measurements of wave packet formation and coherent movement along the excited state and charge-separated state potential surfaces of the reaction center using coherent femtosecond spectroscopy.[58−60] If this is true, then the effective temperature of the vibrational modes coupled to electron transfer (some measure of the energy available in the promoting modes) is not the same as the bath temperature, and in fact becomes largely temperature independent, as is observed. This conclusion is in agreement with previous experiments on the excitation wavelength dependence of energy transfer and initial charge separation in R-26 reaction centers (a carotenoidless mutant) that imply that initial electron transfer occurs before vibrational relaxation is complete.[61]

In fact, it is possible to refit the data of Figure 3, asking what is the effective temperature of the dominant vibrational mode coupled to electron transfer, holding the free energy difference for the wild-type reaction center constant. In this case, the fit is as good as when the free energy difference for the wild-type reaction is allowed to vary. When the standard reaction free energy for the initial electron-transfer reaction is set at −60 meV, the effective temperature of the vibrational mode coupled to electron transfer is found to be 529 K, the reorganization energy is found to be 210 meV, and the coupling term is 33 cm^{-1}. Furthermore, a substantially elevated effective temperature is obtained for any fit assuming a driving force for wild type of less than 200 meV. If indeed the initial reaction has a driving force less than 200 meV (and if $P^+B_B^-$ is the initial charge-separated state, the reaction free energy would have to be less than 200 meV according to any reasonable estimate), this suggests that there could be substantial energy in the vibrational modes coupled to electron transfer above that provided by the thermal bath, explaining the temperature independence of the initial electron-transfer reaction.

Why Is Wild Type Not Optimized for the Highest Rate of Electron Transfer? Wild-type reaction centers of *Rb. sphaeroides*, just as in *Bl. viridis*[13] are not completely optimized in terms of the maximal electron-transfer rate leading to the initial charge-separated state. Further, only minimal protein modifications are necessary to improve this rate by forty percent (the factor is even larger in *Bl. viridis*). The low potential mutants were capable of photosynthetic growth with doubling times comparable to wild type, though a comprehensive range of conditions (light intensities, wavelengths, and temperatures) was not investigated and there may well be growth disadvantages associated with the mutants that were either too small for these methods to measure or which manifest themselves under conditions not tested. In any case, evolutionary pressure must be acting upon some facet of the overall growth of this species other than just the rate of initial electron transfer. Of course, there are other reactions in addition to initial electron transfer that depend on the P/P^+ potential. The free energies of $P^+Q_A^-$ and $P^+Q_B^-$ are lower in the low potential mutants than in wild type and therefore less of the initial photon energy is conserved. It is ultimately the free energy conserved at this point that drives the generation of proton motive force. Thus, decreasing the midpoint potential of P decreases the amount of energy conserved by the electron-transfer chain that is available to drive proton pumping. Wild-type A-side electron-transfer energetics may therefore be a happy medium that preserves a sufficiently fast initial electron transfer to ensure a high quantum yield of initial photochemistry without unduly sacrificing the overall energy conservation of the long-lived charge-separated states.

Acknowledgment. The authors would like to thank J. Dalsing and D. Smith for technical help in constructing some of the mutations. This work was supported by the National

Science Foundation (Grants MCB9817388, MCB0131766 and BIR9512970) and the United States Department of Agriculture (Grant 1999-01753). ALMH was supported by a graduate research training grant from the National Science Foundation (DGE9553456). This is publication #508 from the Center for the Study of Early Events in Photosynthesis.

References and Notes

(1) Allen, J. P.; Feher, G.; Yeates, T. O.; Komiya, H.; Rees, D. C. *Proc. Nat. Acad. Sci. U.S.A.* **1987**, *84*, 5730−5734.

(2) Allen, J. P.; Feher, G.; Yeates, T. O.; Komiya, H.; Rees, D. C. *Proc. Nat. Acad. Sci. U.S.A.* **1988**, *85*, 8487−8491.

(3) Kirmaier, C.; Holten, D.; Parson, W. W. *Biochim. Biophys. Acta* **1985**, *810*, 49−61.

(4) Kirmaier, C.; Holten, D.; Parson, W. W. *Biochim. Biophys. Acta* **1985**, *810*, 33−48.

(5) Allen, J. P.; Williams, J. C. *Bioenerg. Biomembr.* **1995**, *27*, 275−283.

(6) Gunner, M. *Curr. Top. Bioenerg.* **1991**, *16*, 319−367.

(7) Murchison, H. A.; Alden, R. G.; Allen, J. P.; Peloquin, J. M.; Taguchi, A. K. W.; Woodbury, N. W.; Williams, J. C. *Biochemistry* **1993**, *32*, 3498−3505.

(8) Williams, J. C.; Alden, R. G.; Murchison, H. A.; Peloquin, J. M.; Woodbury, N. W.; Allen, J. P. *Biochemistry* **1992**, *31*, 11029−11037.

(9) Woodbury, N. W.; Peloquin, J. M.; Alden, R. G.; Lin, X.; Lin, S.; Taguchi, A. K. W.; Williams, J. C.; Allen, J. P. *Biochemistry* **1994**, *33*, 8101−8112.

(10) Woodbury, N. W.; Lin, S.; Lin, X.; Peloquin, J. M.; Taguchi, A. K. W.; Williams, J. C.; Allen, J. P. *Chem. Phys.* **1995**, *197*, 405−421.

(11) Williams, J. C.; Steiner, L. A.; Feher, G.; Simon, M. I. *Proc. Nat. Acad. Sci. U.S.A.* **1984**, *81*, 7303−7307.

(12) Williams, J. C.; Steiner, L. A.; Ogden, R. C.; Simon, M. I.; Feher, G. *Proc. Nat. Acad. Sci. U.S.A.* **1983**, *80*, 6505−6509.

(13) Arlt, T.; Bibikova, M.; Penzkofer, H.; Oesterhelt, D.; Zinth, W. *J. Phys. Chem.* **1996**, *100*, 12060−12065.

(14) Marcus, R. A. J. *Chem. Phys.* **1956**, *24*, 966.

(15) Woodbury, N.; Allen, J. P. Electron Transfer in Purple Nonsulfur Bacteria. In *Anoxygenic Photosynthetic Bacteria*; Blankenship, R. E., Madigan, M. T., Bauer, C. E., Eds.; Kluwer Academic Publishers: Boston, 1995; Vol. 2; pp 527−557.

(16) Lancaster, C. R. D.; Bibikova, M. V.; Sabatino, P.; Oesterhelt, D.; Michel, H. *J. Biol. Chem.* **2000**, *275*, 39364−39368.

(17) Williams, J. C.; Haffa, A. L. M.; McCulley, J. L.; Woodbury, N. W.; Allen, J. P. *Biochemistry* **2001**, *40*, 15403−15407.

(18) Katilius, E.; Turanchik, T.; Lin, S.; Taguchi, A. K. W.; Woodbury, N. W. *J. Phys. Chem. B.* **1999**, *103*, 7386-7389.

(19) Kirmaier, C.; He, C.; Holten, D. *Biochemistry* **2001**, *40*, 12132−12139.

(20) Katilius, E.; Katiliene, Z.; Lin, S.; Taguchi, A. K. W.; Woodbury, N. W. *J. Phys. Chem. B.* **2002**, *106*, 1471−1475.

(21) Williams, J. C.; Woodbury, N. W.; Taguchi, A. K. W.; Peloquin, J. M.; Murchison, H. A.; Alden, R. G.; Allen, J. P. Mutations That Affect the Donor Midpoint Potential in Reaction Centers from *Rhodobacter sphaeroides*. In *The Photosynthetic Bacterial Reaction Center II. Structure, Spectroscopy and Dynamics*; Breton, J., Vermeglio, A., Eds.; Plenum Press: New York, 1992; pp 25−31.

(22) Williams, J. C.; Taguchi, A. K. W. Genetic Manipulation of Purple Photosynthetic Bacteria. In *Anoxygenic Photosynthetic Bacteria*; Blankenship, R. E., Madigan, M. T., Bauer, C. E., Eds.; Kluwer Academic Publishers: Dordrecht, 1995; Vol. 2; pp 1029−1065.

(23) Paddock, M. L.; Rongey, S. H.; Feher, G.; Okamura, M. Y. *Proc. Nat. Acad. Sci. U.S.A.* **1989**, *86*, 6602−6606.

(24) Goldsmith, J.; Boxer, S. *Biochim. Biophys. Acta* **1996**, *1276*, 171−175.

(25) Straley, S. C.; Parson, W. W.; Mauzerall, D. C.; Clayton, R. K. *Biochim. Biophys. Acta* **1973**, *305*, 597−609.

(26) Van der Rest, M.; Gingras, G. *J. Biol. Chem.* **1974**, *249*, 6446−6453.

(27) Freiberg, A.; Timpmann, K.; Lin, S.; Woodbury, N. W. *J. Phys. Chem. B.* **1998**, *102*, 10974−10982.

(28) Okamura, M. Y.; Isaacson, R. A.; Feher, G. *Proc. Nat. Acad. Sci. U.S.A.* **1975**, *72*, 3491−3495.

(29) Greene, B. I.; Farrow, R. C. *Chem. Phys. Lett.* **1983**, *98*, 273−276.

(30) Freiberg, A.; Timpmann, K.; Ruus, R.; Woodbury, N. W. *J. Phys. Chem. B.* **1999**, *103*, 10032−10041.

(31) Heller, B. A.; Holten, D.; Kirmaier, C. *Science* **1995**, *269*, 940−945.

(32) Kalman, L.; LoBrutto, R.; Allen, J. P.; Williams, J. C. *Nature* **1999**, *402*, 696−699.

(33) Steffen, M. A.; Lao, K.; Boxer, S. G. *Science* **1994**, *264*, 810−816.

(34) Warshel, A.; Parson, W. W. *J. Am. Chem. Soc.* **1987**, *109*, 6143−6152.

(35) Warshel, A.; Parson, W. W. *J. Am. Chem. Soc.* **1987**, *109*, 6452−6163.

(36) Lancaster, C. R. D.; Bibikova, M. V.; Sabatino, P.; Oesterhelt, D.; Michel, H. *J. Biol. Chem.* **2000**, *275*, 39364−39368.

(37) Gray, K. A.; Farchaus, J. W.; Wachtveitl, J.; Breton, J.; Oesterhelt, D. *EMBO J.* **1990**, *9*, 2061−2070.

(38) Kirmaier, C.; Weems, D.; Holten, D. *Biochemistry* **1999**, *38*, 11516−11530.

(39) Roberts, J. A.; Holten, D.; Kirmaier, C. *J. Phys. Chem. B.* **2001**, *105*, 5575−5584.

(40) Bixon, M.; Jortner, J.; Michel-Beyerle, M. E. *Chem. Phys.* **1995**, *197*, 389−404.

(41) Nagarajan, V.; Parson, W. W.; Davis, D.; Schenck, C. C. *Biochemistry* **1993**, *32*, 12324−12336.

(42) Jortner, J. *Chem. Phys.* **1976**, *64*, 4860−4867.

(43) Hopfield, J. *Proc. Nat. Acad. Sci. U.S.A.* **1974**, *71*, 3640−3644.

(44) Marcus, R. A.; Sutin, N. *Biochim. Biophys. Acta* **1985**, *811*, 265−322.

(45) Ogrodnik, A.; Volk, M.; Letterer, R.; Feick, R.; Michel-Beyerle, M. E. *Biochim. Biophys. Acta* **1988**, *936*, 361−371.

(46) Chidsey, C. E. D.; Takiff, L.; Goldstein, R. A.; Boxer, S. G. *Proc. Nat. Acad. Sci. U.S.A.* **1985**, *82*, 6850−6854.

(47) Peloquin, J. M.; Williams, J. C.; Lin, X.; Alden, R. G.; Murchison, H. A.; Taguchi, A. K. W.; Allen, J. P.; Woodbury, N. W. *Biochemistry* **1994**, *33*, 8089−8100.

(48) Volk, M.; Aumeier, G.; Langenbacher, T.; Feick, R.; Ogrodnik, A.; Michel-Beyerle, M.-E. *J. Phys. Chem. B.* **1998**, *102*, 735−751.

(49) Schenck, C. C.; Blankenship, R. E.; Parson, W. W. *Biochim. Biophys. Acta* **1982**, *680*, 44−59.

(50) Woodbury, N. W. T.; Parson, W. W. *Biochim. Biophys. Acta* **1984**, *767*, 345−361.

(51) Zusman, L. D.; Beratan, D. N. *Spectrochim. Acta, A* **1998**, *54*, 1211−1218.

(52) Hoff, A. J.; Deisenhofer, J. *Phys. Rep.−Rev. Sect. Phys. Lett.* **1997**, *287*, 2−247.

(53) Moser, C. C.; Dutton, P. L. Outline of Theory of Protein Electron Transfer. In *Protein Electron Transfer*; Bendall, S. D., Ed.; BIOS Scientific Publishers: Ltd.: Oxford, 1996; pp 1−21.

(54) Hales, B. J. *Biophys. J.* **1976**, *16*, 471−480.

(55) Woodbury, N. W.; Lin, S.; Lin, X.; Peloquin, J. M.; Taguchi, A. K. W.; Williams, J. C.; Allen, J. P. *Chem. Phys.* **1995**, *197*, 405−421.

(56) Maroti, P.; Hanson, D. K.; Baciou, L.; Schiffer, M.; Sebban, P. *Proc. Nat. Acad. Sci. U.S.A.* **1994**, *91*, 5617−5621.

(57) Ivancich, A.; Mattioli, T. A.; Artz, K.; Wang, S.; Allen, J. P.; Williams, J. C. *Biochemistry* **1997**, *36*, 3027−3036.

(58) Vos, M. H.; Rischel, C.; Jones, M. R.; Martin, J.-L. *Biochemistry* **2000**, *39*, 8353−8361.

(59) Yakovlev, A. G.; Shkuropatov, A. Y.; Shuvalov, V. A. *FEBS Lett.* **2000**, *466*, 209−212.

(60) Yakovlev, A. G.; Shkuropatov, A. Y.; Shuvalov, V. A. *Biochemistry* **2002**, *41*, 2667−2674.

(61) Lin, S.; Taguchi, A. K. W.; Woodbury, N. W. *J. Phys. Chem.* **1996**, *100*, 17067−17078.

(62) Williams, J. C.; Alden, R. G.; Coryell, V. H.; Lin, X.; Murchison, H. A.; Peloquin, J. M.; Woodbury, N. W.; Allen, J. P. Changes in the Oxidation Potential of the Bacteriochlorophyll Dimer Due to Hydrogen Bonds in Reaction Centers from *Rhodobacter sphaeroides*. In *Research in Photosynthesis*; Murata, N., Ed.; Kluwer Academic Publishers: Dordrecht, 1992; Vol. I, pp 377−380.